REVISTA MATÉRIA V.28 N.3
ISSN 1517-7076 articles e20230165, 2023

Corrosion of galvanic couples of stainless steels with non-precious alloys in the oral cavity

Elvar Quezada-Castillo[1], Wilder Aguilar-Castro[1], Bertha Quezada-Alván[2]

[1]Universidad Nacional de Trujillo, Departamento Académico de Física, Laboratorio de Física de Materiales "Lennart Hasselgren". Ciudad Universitaria, 13001, Trujillo, La Libertad, Perú.

[2]Universidad Privada Antenor Orrego, Departamento de Ciencias. Av. América Sur, 3145, Monserrate, 13001, Trujillo, La Libertad, Perú.

e-mail: elvarq@yahoo.es, wilderag@yahoo.com, quezada_b@yahoo.es

ABSTRACT

In the restoration of lost or misaligned dental pieces, dissimilar dental alloys are frequently used in the oral cavity, which form galvanic couples that corrode due to the effect of saliva and dentin fluids. In this work, the microstructure of ten non-precious dental alloys was analyzed by optical microscopy, the open-circuit corrosion potential of each alloy was measured against a saturated calomel electrode, they were subjected to accelerated corrosion processes in aerated artificial saliva and plotted the potentiodynamic polarization curves of these alloys. Then, the corrosion potential and current density of the galvanic couples formed by stainless steels 304 and 316L with non-precious dental alloys of Ni-Cr, Co-Cr, and Cu base alloys (Cu-Ni, Cu-Zn and Cu-Al), using the Evans method whose results were not compatible with the principle of galvanic couples, so the Mansfeld equations were used with which results consistent with the aforementioned principle were obtained.

Keywords: Non-precious dental alloys; galvanic couples; artificial saliva; polarization curves.

1. INTRODUCTION

Dental alloys for casting and casting are available on the market in a wide variety of compositions and with suitable mechanical and electrochemical properties to fulfill functions of use in inlays, crowns, bridges, partial and total dentures, brackets and implants [1, 2]. The most traditional are the noble alloys that contain not less than 75% gold and platinum group metals; these alloys do not deteriorate in their properties over time nor do they lose their aesthetic appearance [3, 4]. However, they have high density, low elastic modulus and are excessively expensive. For this reason and to replace alloys with a high gold content, non-precious alloys have been developed, which have been used since the 1940s in developed countries such as the United States, Germany, France and Japan. Among these alloys are those of Co-Cr, Ni-Cr, stainless steel, titanium-based alloys [5–9] and in the last decades of the last century, copper-based alloys in developing countries in the Middle East and America South (Brazil, Argentina and Peru) in order to lower costs and make prostheses accessible to low-income people [10–15]. To avoid the indiscriminate use of these alloys, electrochemical corrosion studies were carried out in corrosive media that simulate the oral cavity in order to typify the existing alloys in the national and international market, implementing and disseminating their true properties among users and not those that are disclosed the marketing chains [16].

Dental restorations frequently require the use of dissimilar alloys in the oral cavity, as in the case of a tooth filled with amalgam coming into direct, indirect or intermittent contact with another tooth restored with a different alloy, giving rise to oral galvanism due to electrical currents that flow between these alloys through saliva and fluids of oral and dentinal tissues [17, 18]. Oral galvanism produces different effects such as headache, metallic taste, fainting, nausea, burning sensation of the tongue, and unusually dry mouth [19, 20].

For this reason, we will study the corrosion of galvanic couples of stainless steels 304 and 316L with non-precious dental alloys of Ni-Cr, Co-Cr, Cu-Ni, Cu-Zn and Cu-Al in aerated artificial saliva using the method Evans and Mansfeld formulas and by optical microscopy we will analyze the microstructure of the alloys used in this work.

Corresponding Author: Wilder Aguilar-Castro Received on 27/05/2023 Accepted on 17/07/2023

DOI: https://doi.org/10.1590/1517-7076-RMAT-2023-0165

2. MATERIALS AND METHODS

2.1. Materials

Ten non-precious dental alloys were used: two 304 and 316L stainless steels, two Ni-Cr alloys, two Co-Cr alloys and four Cu-based alloys whose chemical composition and trade names are shown in Table 1.

2.2. Specimen preparation

- The specimens of the copper, Co-Cr and Ni-Cr base alloys were prepared by the lost wax method with an oxygen-butane-propane flame, and by a centrifugation process [22]. The test pieces consisted of sheets with a surface area of 1 cm × 1 cm and a thickness of 0,20 cm.
- The stainless steel specimens (in sheets and wires) were prepared by cutting pieces of the "as-received" material to expose a surface area of 1 cm^2 to the solution.

2.3. Revealing of microstructures

To reveal the microstructure of the tested materials, the specimens were prepared metallographically by polishing them with silicon carbide papers of different granulometry, from 220 to 2000, and then with diamond paste up to 0.25 μm.

The development of the microstructure was carried out by attacking them with the following solutions [23]:

- SS 304, SS 316L, Co-Cr y Ni-Cr with the reagent: HCl (20 mL), HNO_3(10 mL), $FeCl_3$(3 g) from 5 to 30 seconds.
- Cu-Ni, Cu-Zn y Cu-Al with the reagent: HCl (20 mL), H_2O (100 mL), $FeCl_3$(5–10 g) from 5 to 10 seconds.

2.4. Electrochemical corrosion tests

To determine the corrosion current density of galvanic couples in artificial saliva, corrosion potential measurements were made and the polarization curves of the alloys under study were determined.

2.4.1. Corrosion potential measurements

Open-circuit corrosion potential (OCP) was measured with a saturated calomel electrode (SCE) in a three-electrode cell with a Princeton Applied Research model 173 potentiostat in aerated artificial saliva at 25 ºC. Measurements were made in triplicate with different specimens of each alloy, previously allowing the potential to stabilize for one hour in the solution, continuously aerating it with a fish tank aerator at approximately 80 bubbles per minute.

2.4.2. Polarization curves

Polarization curves in aerated artificial saliva were plotted in triplicate using the same cell and potentiostat as that used to measure OCP. The reference electrode was also saturated calomel and the counter electrode was

Table 1: Chemical composition of dental alloys used in the present study in mass % [21].

MATERIAL	CHEMICAL COMPOSITION (% m/m)
316L Stainless Steel (Fe-Cr-Ni)	Fe 65,20 - Cr 17,00 - Ni 13,00 - Mo 2,50 - Mn 2,00 - C < 0,08
304 Stainless Steel (Fe-Cr-Ni)	Fe 73,90 - Cr 16,00 - Ni 8,00 - Si 0,70 - Mo 0,40 - C 0,08
Verabond 2 (Ni-Cr)	Ni 77,00 - Cr 12,50 - Mo 4,30 - Nb 4,00 - Al 2,30
Verabond (Ni-Cr)	Ni 77,90 - Cr 12,60 - Mo 5,00 - Be 1,90 - Al 2,60
Vera PDN (Co-Cr)	Co 63,00 - Cr 27,00 - Mo 5,50 - Fe 2,00 - Ni 1,00
Supercrom (Co-Cr)	Co 62,50 - Cr 30,00 - Mo 6,00
Platcast (Cu-Ni)	Cu 65,00 - Ni 30,00 - Al 5,00
Oropent (Cu-Zn)	Cu 54,10 - Zn 45,70 - Fe 0,05 - Ni 0,02
Pentacast (Cu-Al)	Cu 77,90 - Al 12,00 - Ni 5,10 - Fe 5,00
Orcast Soft (Cu-Al)	Cu 77,00 – Al 6,50 - Zn 12,50 - Ni 4,00

platinum. The scanning speed was 12 mV/min controlled with a Universal PAR 175 Programmer and the curves were recorded with an XT PAR model REO 151 plotter. Before starting the curves, the corrosion potential of the surface was measured. same way as in the previous section. The anodic and cathodic curves of each alloy were drawn separately with different specimens starting from the OCP.

2.4.3. Corrosion potentials of galvanic couples

Dental alloys corrode in the mouth due to the action of saliva and dentin fluids, so that when electrically coupled they polarize and corrode at a new speed. When metals A and B are coupled, the mixed potential of the galvanic couple, E_{cupla} ($V_{corr.PG}$), is found at the intersection of the polarization curves where the total oxidation rate is equal to the total reduction rate and the polarization current density is I_{couple} (or $I_{corr.PG}$) [24]. This process that allows to determine the potential and current density of the galvanic couple is called Evans method.

2.5. Electrolyte

The electrolyte used in the potentiodynamic tests was an experimental saliva [11, 12] that reproduces the electrochemical behavior of natural saliva, whose composition in grams per liter (g/L) is:

NaCl(0,600), KCl(0,720), $CaCl_2 \cdot 2H_2O$(0,220), KH_2PO_4(0,680), $Na_2HPO_2 \cdot 12H_2O$(0,856), KSCN(0,060), $KHCO_3$(1,500) and $H_8C_6O_7$(0,030), prepared with deionized water of 18,20 MΩ-cm electrical resistivity and with analytical grade reagents. The pH of the solution was 6,5; to prevent this value from being modified, $KHCO_3$ must be added shortly before starting the tests.

3. RESULTS AND DISCUSSION

3.1. Metallographic analysis

- Figures 1A and 1B show the microstructures of 304 and 316L austenitic stainless steels. The first corresponds to a sheet of the material in which equiaxed grains with twins inside can be seen, while the second (wire) shows a totally deformed structure due to the drawing of the material.
- Figures 2A and 2B show the microstructures of the Ni-Cr alloys: Verabond and Verabond 2. In the Verabond alloy, the dendritic structure (light part) is immersed in a eutectic structure due to the presence of the NiBe and α – NiCrMo phases (matrix material) and from the literature it is known that the size of the eutectic increases with Be content [25, 26]. The dendritic structure of these alloys is a solid solution rich in Ni, as can be deduced from the chemical composition of the alloy and the corresponding phase diagram.
- Figures 3A and 3B show the microstructure of Vera PDN and Supercrom Co-Cr alloys, which are solid solutions of chromium in cobalt with complex carbides in the interstices of the dendrites. Complex carbides include Cr_4C, Cr_7C, $Cr_{23}C$, MC, and M_6C, where M can be an element such as niobium, titanium, tantalum, or tungsten [26, 27].
- Figure 4A and 4B shows the microstructures of Platcast (Cu-Ni) and oropent (Cu-Zn) alloys. Platcast is a Ni-rich solid solution as deduced from its composition and phase diagram. Oropent is characterized by the presence of large polygonal grains and is classified in the group of β brasses [28].
- Figures 5A and 5B show the microstructure of the Cu-Al and Cu-Zn alloys: Pentacast and Orcast Soft (with small amount of Zn). In them, the presence of dendrites (clear areas) immersed in an interdendritic region is observed. These zones correspond to the α phase, which is a solid solution of aluminum in copper, and the interdendritic zones formed by the β phase, stable at high temperatures, which below 580 ºC gives rise to the α and γ_2 phases [29].

3.2. Corrosion potentials

Table 2 shows the open-circuit corrosion potentials (OCP) of the alloys under study, ordered according to their corrosion potential from least to most, forming an electrochemical series in aerated artificial saliva. The average standard deviation of the OCP calculated according to the G:16-95 ASTM standard [30] is also shown.

The most active dental alloy is Orcast Soft, whose corrosion potential is –0,270 V_{sce}. This alloy will always be anode when it forms galvanic pairs with any of the copper-based dental alloys and stainless steels considered in this work.

3.3. Polarization curves

The polarization curves were determined under static conditions at room temperature (25 ºC). The cathodic curves of the alloys under study are all similar because at small cathodic overpotentials the current density

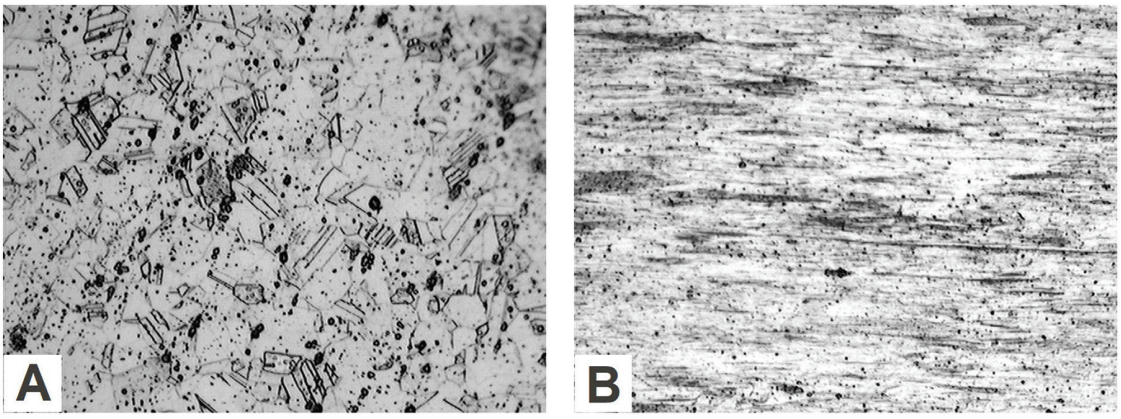

Figure 1: Optical micrographs of the microstructure of (A) 304 stainless steel and (B) 316L stainless steel at 100×.

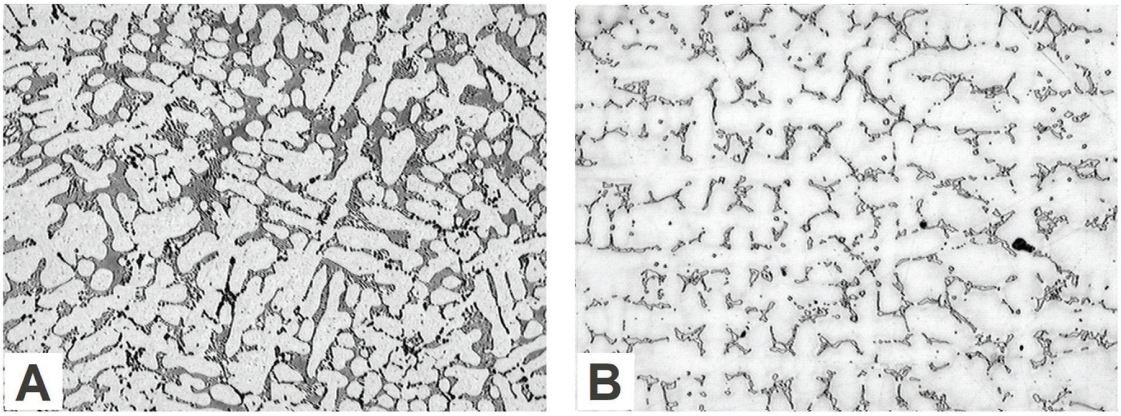

Figure 2: Optical micrographs of the microstructure of (A) Verabond and (B) Verabond 2 at 100×.

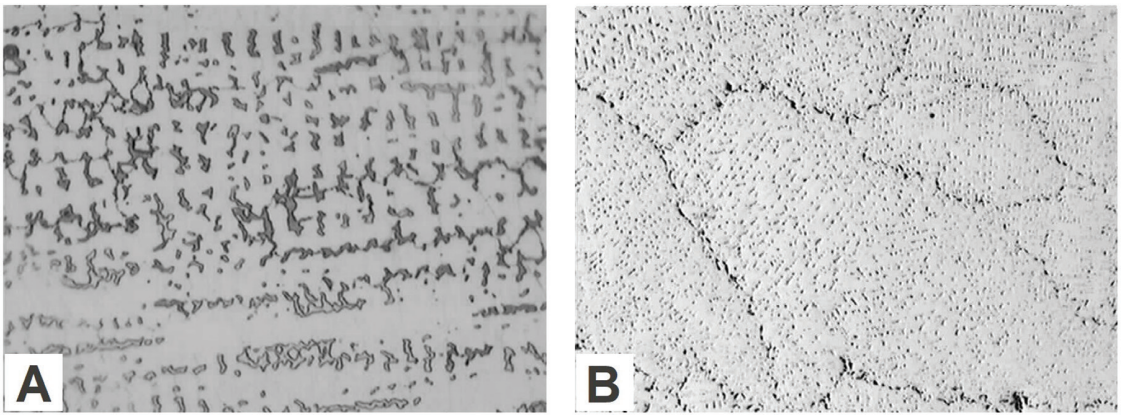

Figure 3: Optical micrographs of the microstructure of (A) Vera PDN and (B) Supercrom at 100×.

increases rapidly, observing a linear relationship between the overpotential and the logarithm of the current. In all cases the cathodic region corresponds to the evolution of hydrogen and reduction of oxygen [31].

The polarization curves of 304 and 316L stainless steels in artificial saliva are shown in Figure 6. The passive zone of 304 stainless steel extends from –0,080 V_{sce} to 0,430 V_{sce} with a current density of 0,60 μA/cm^2. The passivation rupture potential is 0,450 V_{sce} due to the pitting of the material produced by the chlorides in the solution. The passive zone of 316L stainless steel extends from –0,050 V_{sce} to 1,060 V_{sce} with a current density of 0,790 μA/cm^2. From this potential, the current density increases due to the nucleation of pits or pits around the

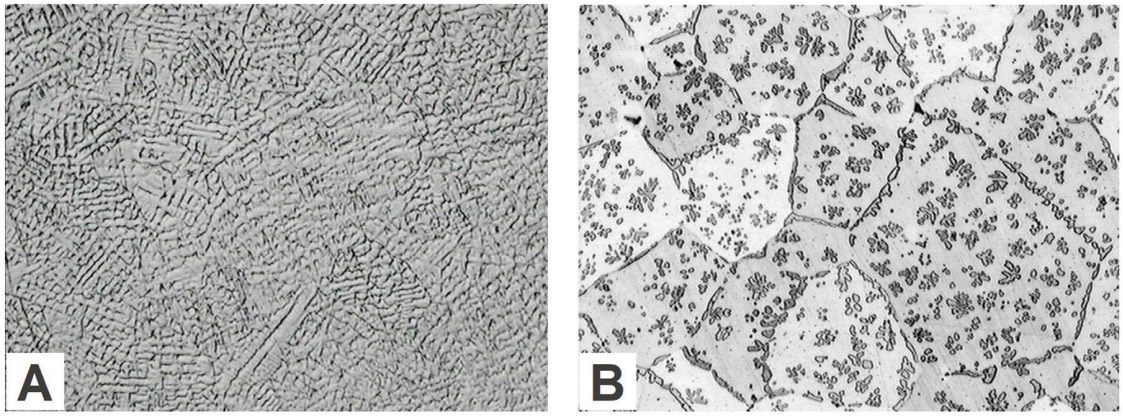

Figure 4: Optical micrographs of the microstructure of (A) Platcast and (B) Oropent at 100×.

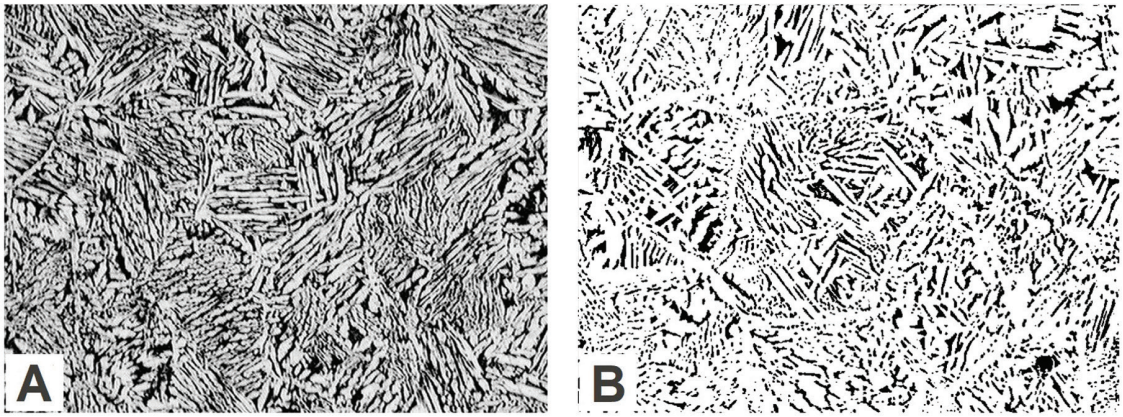

Figure 5: Optical micrographs of the microstructure of Pentacast (A) and Orcast Soft (B) at 100×.

Table 2: Open-circuit corrosion potentials and intensities of dental alloys under study in aerated artificial saliva.

MATERIALS	NOTATION	V_{corr} (V_{sce})	I_{corr}(μA/cm²)
Stainless steel 316L	1	–0,061 ± 0,011	0,034
Stainless steel 304	2	–0,180 ± 0.016	0,124
Verabond 2 (Ni-Cr)	3	–0,185 ± 0,006	0,180
Verabond (Ni-Cr)	4	–0,192 ± 0,005	0,235
Vera PDN (Co-Cr)	5	–0.216 ± 0.007	0.110
Supercrom (Co-Cr)	6	–0,244 ± 0,012	0,508
Platcast (Cu-Ni)	7	–0,250 ± 0,005	0,073
Oropent (Cu-Zn)	8	–0,253 ± 0,011	0,440
Pentacast (Cu-Al)	9	–0,260 ± 0,007	1,720
Orcast Soft (Cu-Al)	10	–0,270 ± 0,004	1,000

existing inclusions on the surface of the sample. If there were no inclusions for the pitting to nucleate, the pitting potential would be higher due to the high passivity of the metal. The presence of Fe, Cr, Cl, and oxygen in the passive layer of 316L stainless steel in solutions containing NaCl, such as saliva, is attributed to the formation of Fe_2O, Cr_2O_3, and FeCl according to EDX analysis by REFAEY *et al*. [32].

The greater resistance to corrosion of SS 316L compared to 304 stainless steel is due to the greater amount of chromium and molybdenum it contains and its biocompatibility makes it a useful material for medical applications, orthopedic implants and orthodontic appliances such as arch wires, brackets, bands, ligatures,

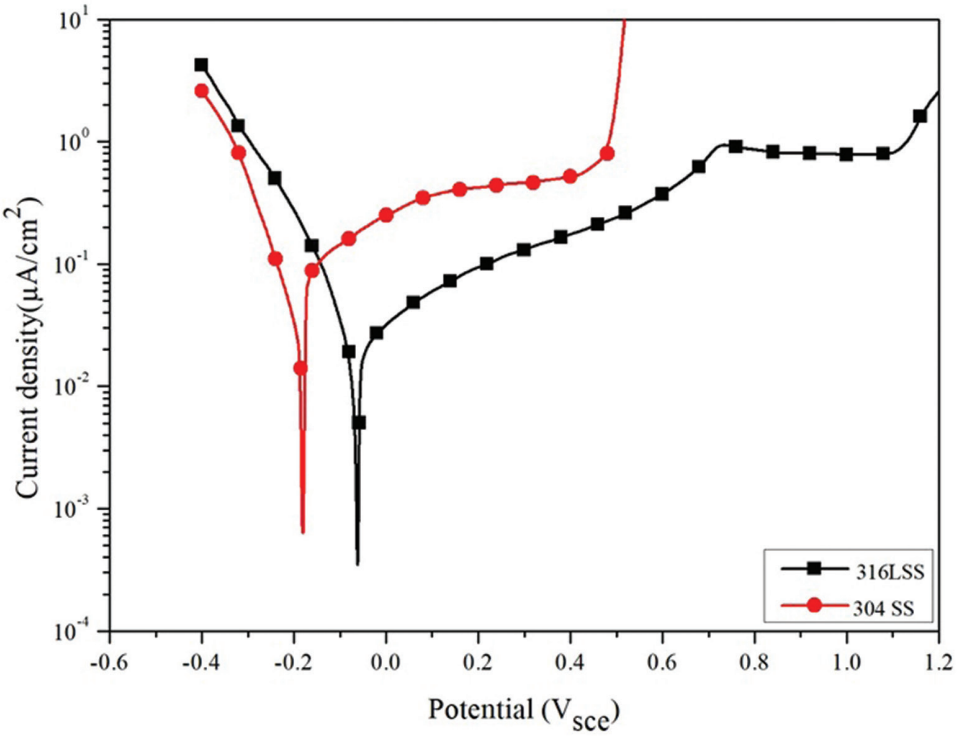

Figure 6: Potentiodynamic polarization curves of 304 and 316L stainless steels in aerated artificial saliva.

tubes, dental crowns among others [33, 34]. Thanks to molybdenum, it is ideal for cutting edges such as scalpels, medical needles, medical syringes, etc. Among other applications, it is also used for orthopedic implants, screws and bone fixation plates.

The 304 stainless steel has the same applications as SS 316L with some restrictions and is used for the manufacture of medical devices which do not chemically react with body tissue due to its high corrosion resistance and low carbon. The nickel contained in these steels provides an extremely smooth and polished surface, giving it the fine details necessary for precision mixing.

Figure 7 shows the polarization curves of the Ni-Cr and Co-Cr alloys. The passive zone of Verabond 2 alloy extends from –0,040 V_{sce} to 0,510 V_{sce} with an average passivation current density of 0,760 μA/cm². The Verabond passive zone extends from –0,100 V_{sce} to 0,130 V_{sce} with an average current density in that zone of 0,60 μA/cm². The passive zone of Vera PDN extends from 0,100 V_{sce} to 0,440 V_{sce} with an average current density of 0,29 μA/cm² in this zone. For Supercrom, the passive zone extends from –0,180 V_{sce} to 0,520 V_{sce} with an average current density in that zone of 0,55 μA/cm². The corrosion current densities of the alloys under study increase rapidly from their rupture potential, due to the dissolution of the interdendritic zone by the presence of Cr and Mo precipitates (mainly Mo) [35, 36]. In general, the corrosion resistance of Co-Cr alloys is due to the presence of the Cr (III) oxide-hydroxides present in the passive layers of these alloys [37].

In general, Ni-Cr and Co-Cr alloys are used in prosthodontics for crowns and bridges, as well as post-core constructions with some concerns about the toxic and allergic effect of nickel on the human body when exposed in the oral cavity. Co-Cr is a biocompatible alloy that is also used for metal-ceramic restorations because plastic deformation and porcelain detachment are rare due to its high elastic limit [38].

The polarization curves of copper-based dental alloys are shown in Figure 8. The Cu-Ni alloy (Platcast) has a passive zone that extends from –0,180 V_{sce} to 0,250 V_{sce} with an average passivation current density of 0,560 μA/cm² approx. The Cu-Zn alloy (Oropent) has a passive zone that extends from –0,160 to 0,040 V_{sce} and an average current density in that zone of 1,90 μA/cm²; this small passive zone is due to its high Zn content [18]. The passive zone of Cu Al alloys extends from –0,180 V_{sce} to 0,120 V_{sce} for Orcast Soft and up to 0,180 V_{sce} for Pentacast with average passivation current densities of 1,35 μA/cm² and 1,45 μA/cm², respectively. From the rupture potentials, the corrosion current densities of the alloys under study increase rapidly to small over potentials as shown in the figure above, due to the selective dissolution of the material, a phenomenon known as dealloying.

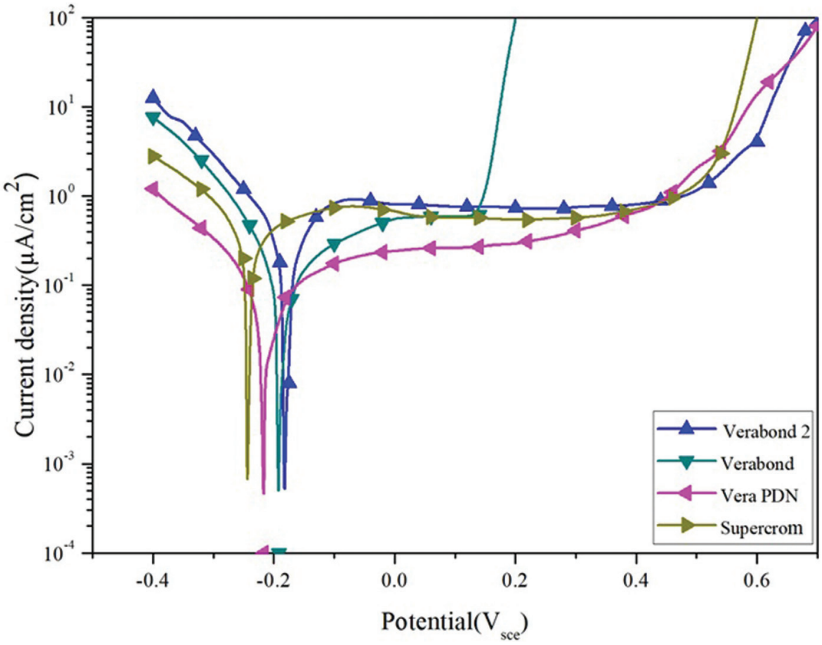

Figure 7: Potentiodynamic polarization curves of Co-Cr and Ni-Cr dental alloys in aerated artificial saliva.

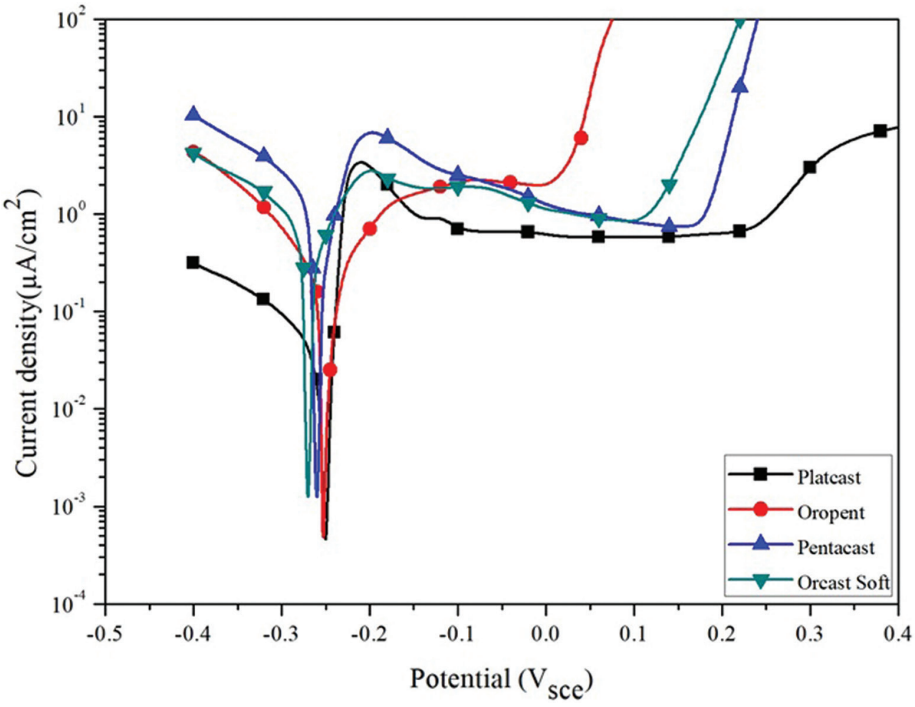

Figure 8: Potentiodynamic polarization curves of copper-based dental alloys in aerated artificial saliva.

Cu-Ni and Cu-Al alloys are used to fabricate full cast crowns, inlays, short-span multi-unit bridges, dental posts and cores, metal substructures for veneer crowns using polymer resins [21]. Oropent dental alloy is used in pontics, bridges, inlays, posts and dental crowns [39].

3.4. Corrosion potentials and current densities of galvanic couples of dental alloys

The instantaneous corrosion potentials and current densities of the galvanic couples between different materials are obtained theoretically using the Evans method described in section 2.4.3. In this case, the cathodic curves

of the 304 and 316L stainless steels are superimposed with the anodic curves of the Ni-Cr, Co-Cr and Cu base alloys as shown in Figures 9 and 10. The red and black squares in the intersection of the cathodic curves of stainless steels 316L and 304 with the anodic curves of non-precious alloys indicate the corrosion potential and current density of the respective galvanic couple. Except for the galvanic couple $PG_{1,2}$ of stainless steels in which 304 stainless steel acts as anode and 316L stainless steel as cathode, intersecting in this case the anodic curve of 304 steel with the cathodic curve of 316L steel. In all cases, 316L stainless steel acts as the cathode.

The corrosion potentials and current densities of the galvanic couples are presented in Tables 3 and 4, observing that: the most susceptible to corrosion are the couples formed between 316L and 304 stainless steels with the Orcast Soft copper-aluminum alloy, and the most resistant to corrosion are the couplings formed between 304 stainless steel and the Ni-Cr and Co-Cr alloys considered in this work.

3.5. Correction of galvanic current density results by the Mansfeld method

In the 70s of the last century, MANSFELD and KENKEL [40], MANSFELD [41, 42] systematically studied the behavior of galvanic couples and the applicability of superimposing Evans diagrams to determine galvanic current densities, reaching the conclusion that three cases must be considered: 1) Tafel behavior, 2) diffusional control and 3) small polarization ranges. In this paper we will deal only with the latter case.

For small polarization ranges, coupling metal A with metal B (more noble than A) produces only a small shift in the corrosion potential of metal A. Therefore, the galvanic couple potential of the two dissimilar metals coupled, is located very close to the corrosion potential of the uncoupled anode and Tafel type behavior does not occur.

In this case, the galvanic current ($I_{corr.PG}$) is not equal to the metal dissolution current A. This last current is the sum of the cathodic currents on the anode ($I_{A,c}$) and on the cathode ($I_{B,c}$):

$$I_{A,a} = I_{A,c} + I_{B,c} \tag{1}$$

while the galvanic current is equal to the cathodic current on metal B:

$$I_{corr.PG} = I_{B,c} = I_{A,a} - I_{A,c} \tag{2}$$

from where

$$I_{A,a} = I_{corr.PG} + I_{A,c} \tag{3}$$

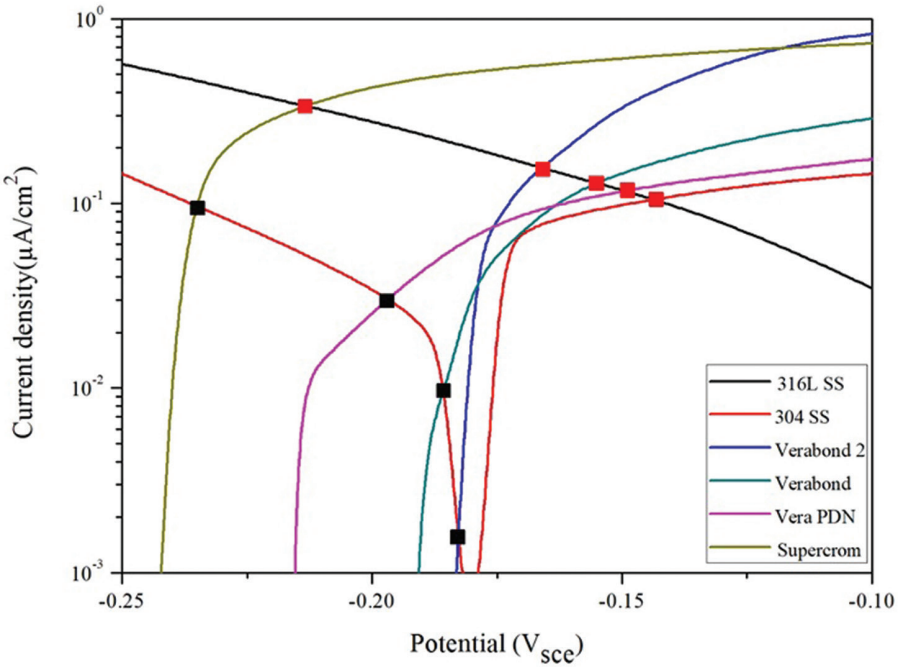

Figure 9: Superposition of cathodic polarization curves for 316L stainless steel, cathodic and anodic polarization curves for 304 stainless steel, and anodic polarization curves for Ni-Cr and Co-Cr alloys in aerated artificial saliva.

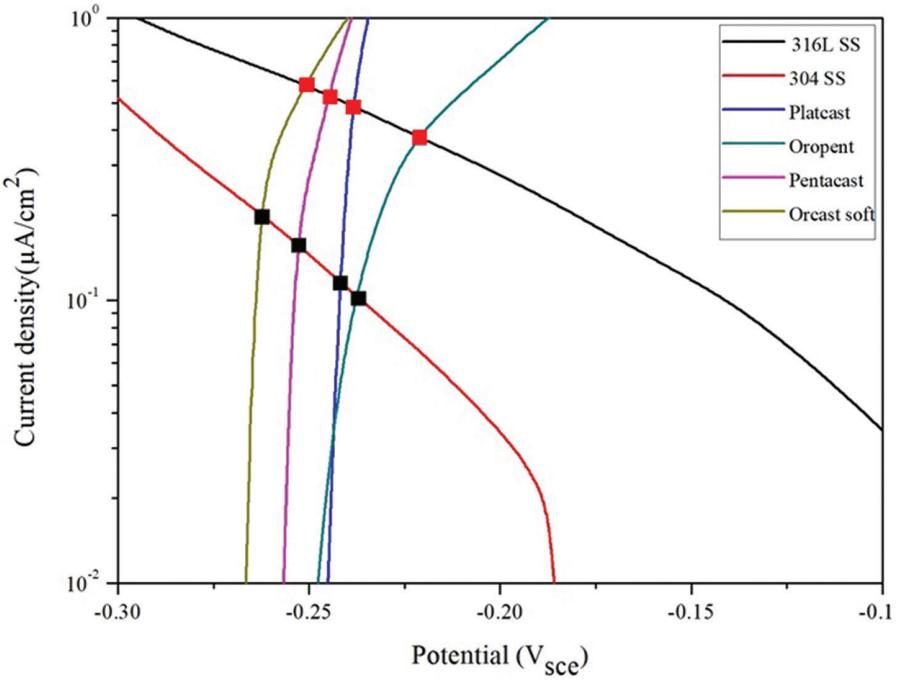

Figure 10: Superposition of cathodic polarization curves of 304 and 316L stainless steel and anodic polarization curves of Cu base alloys in aerated artificial saliva.

Table 3: Corrosion potentials and current density of galvanic couples of non-precious dental alloys with 316L stainless steel.

GALVANIC PAIR	GP	V_{corr}.PG (V_{sce})	I_{corr}.PG (μA/cm²)
316L SS/304 SS	$PG_{1,2}$	–0,143	0,105
316L SS/Verabond 2	$PG_{1,3}$	–0,166	0,156
316L SS/Verabond	$PG_{1,4}$	–0,155	0,130
316L SS/Vera PDN	$PG_{1,5}$	–0,149	0,117
316L SS/Supercrom	$PG_{1,6}$	–0,213	0,334
316L SS/Platcast	$PG_{1,7}$	–0,238	0,473
316L SS/Oropent	$PG_{1,8}$	–0,221	0,373
316L SS/Pentacast	$PG_{1,9}$	–0,245	0,528
316L SS/Orcast Soft	$PG_{1,10}$	–0,250	0,570

The magnitude of the current density of the galvanic couple ($I_{corr.PG}$) is determined with the Evans diagrams and the cathodic current density of anode A is calculated with the formula:

$$I_{A,c} = I_{corr.A} exp\left(-\frac{\left(V_{corr.PG} - V_{corr.A}\right)}{0,434\, b_c}\right) \quad (4)$$

where $V_{corr.PG}$ is the corrosion potential of the galvanic couple, $V_{corr.A}$ and $I_{corr.A}$ are the corrosion potential and the corrosion current density of the uncoupled anode; b_c is the cathodic Tafel slope of the anode material (A).

The polarization range ($V_{corr.PG} - V_{corr,A}$) of the galvanic couples of the copper-based dental alloys with the stainless steels considered in this work is very small, less than 0,20 V_{ecs}, for which the formulas (3) and (4) to determine the true anode solution current density ($I_{A,a}$) at the corrosion potential of the galvanic couple. We will illustrate the calculation of $I_{A,a}$ with an example.

Table 4: Corrosion potentials and current density of galvanic couples of non-precious dental alloys with 304 stainless steel.

GALVANIC PAIR	GP	V_{corr}.PG (V_{sce})	I_{corr}.PG (μA/cm²)
304 SS/Verabond 2	$PG_{2,3}$	–0,183	0,002
304 SS/Verabond	$PG_{2,4}$	–0,185	0,009
304 SS/Vera PDN	$PG_{2,5}$	–0,196	0,030
304 SS/Supercrom	$PG_{2,6}$	–0,235	0,096
304 SS/Platcast	$PG_{2,7}$	–0,242	0,116
304 SS/Oropent	$PG_{2,8}$	–0,237	0,101
304 SS/Pentacast	$PG_{2,9}$	–0,253	0,156
304 SS/Orcast Soft	$PG_{2,10}$	–0,262	0,200

Table 5: Cathodic Tafel slopes, potentials and corrosion current densities of galvanic couples of 304 and 316L stainless steel with copper-based dental alloys by the Evans and Mansfield methods.

ALLOYS	b_c (V_{sce}/decade)	I_{corr} (μA/cm²) (Disengaged)	PG CODE	I_{corr}.PG (μA/cm²) (Evans)	$I_{A,a}$(μA/cm²) (Mansfeld)
SS 316L	0,170	0,034	–	–	–
SS 304	0,165	0,124	$PG_{1,2}$	0,105	0,179
Verabond 2	0,156	0,180	$PG_{1,3}$	0,156	0,292
Verabond	0,132	0,235	$PG_{1,4}$	0,130	0,253
Vera PDN	0,170	0,110	$PG_{1,5}$	0,117	0,161
Supercrom	0,200	0,508	$PG_{1,6}$	0,334	0,689
Platcast	0,237	0,073	$PG_{1,7}$	0,473	0,538
Oropent	0,139	0,440	$PG_{1,8}$	0,373	0,632
Pentacast	0,181	1,720	$PG_{1,9}$	0,528	1,948
Orcast Soft	0,225	1,000	$PG_{1,10}$	0,570	1,384
Verabond 2	0,156	0,180	$PG_{2,3}$	0,002	0,180
Verabond	0,132	0,235	$PG_{2,4}$	0,009	0,217
Vera PDN	0,170	0,110	$PG_{2,5}$	0,030	0,114
Supercrom	0,200	0,508	$PG_{2,6}$	0,096	0,554
Platcast	0,237	0,073	$PG_{2,7}$	0,116	0,183
Oropent	0,139	0,440	$PG_{2,8}$	0,101	0,438
Pentacast	0,181	1,720	$PG_{2,9}$	0,156	1,729
Orcast Soft	0,225	1,000	$PG_{2,10}$	0,200	1,121

For the galvanic couple $PG_{2,9}$ (304 SS/Pentacast), the open circuit corrosion current density (Table 2) is: $I_{corr.PG}$ = 1,720 μA/cm² and the current density $I_{A,c}$ corresponding to the anode (Pentacast) is determined using formula (4) and the data in Tables 2, 4 and 5.

$$I_{9,c} = (1,720\ \mu A/cm^2)\ exp\left(-\frac{-0,253+0,260}{0,434\times 0,181}\right)$$

from where

$$I_{A,c} = I_{9,c} = 1{,}573\ \mu A/cm^2$$

The dissolution of the anode (Pentacast) at the corrosion potential of the $PG_{2,9}$ pair is obtained with formula (3):

$$I_{A,a} = 1{,}729\ \mu A/cm^2$$

In this way, the real values of anode dissolution of the galvanic couples considered in this work were theoretically determined, which are presented in Table 5. This table shows that the corrosion current density of the galvanic couples of the alloys does not precious alloys acting as anodes and stainless steels 304 and 316L as cathodes, evaluated with the Mansfeld formula, are greater than the current densities of non-precious alloys uncoupled according to the PG principle which states that the current density of the galvanic couple ($I_{corr.PG}$) must be greater than the current density ($I_{corr.A}$) of the uncoupled anode [32].

4. CONCLUSIONS

From the results obtained in this work we can conclude:

1. When forming galvanic pairs with copper-based dental alloys, stainless steels 304 and 316L act as cathodes because they have a higher corrosion potential than these alloys in aerated artificial saliva.
2. The most resistant galvanic couples to corrosion in the oral cavity are those formed between stainless steels and Ni-Cr and Co-Cr dental alloys.
3. The experimental results show that for small polarizations, the Evans method does not always give good results to predict the rate of dissolution of the anodic component of the galvanic couples of stainless steels 304 and 316L with non-precious dental alloys in aerated artificial saliva, therefore that it is necessary to use the Mansfeld correction formulas.

5. BIBLIOGRAPHY

[1] ROACH, M., "Base metal alloys used for dental restorations and implants", *Dental Clinics of North America*, v. 51, n. 3, pp. 603–627, vi, Aug. 2007. doi: http://dx.doi.org/10.1016/j.cden.2007.04.001. PubMed PMID: 17586146.

[2] MELO DE MATOS, J.D., *et al*., "Metal alloys in dentistry: an outdated material or required for oral rehabilitation?", *International Journal of Odontostomatology*, v. 15, n. 3, pp. 702–711, 2021. doi: http://dx.doi.org/10.4067/S0718-381X2021000300702

[3] GOLDFOGEL, M.H., NIELSEN, J.P., *Aleaciones para colados dentales: actualización de la terminología*, https://sppdmf.pe/wp-content/uploads/2020/ediciones/1983/aleaciones.pdf, accessed in August, 2022.

[4] AMERICAN DENTAL ASSOCIATION, *Guide to dental materials and devices*, 7th ed., American Dental Association, Chicago, 1974.

[5] ELSHAHAWY, W., WATANABE, I., "Biocompatibility of dental alloys used in dental fixed prosthodontics", *Tanta Dental Journal*, v. 11, n. 2, pp. 150–159, Sep. 2014. doi: http://dx.doi.org/10.1016/j.tdj.2014.07.005

[6] NEAGA, V., BENEA, L., ALEXANDRA, A., "316L stainless steel alloys orthodontic application: effect of fluorinated toothpaste on the corrosion behavior in human saliva", *International Journal of Electrochemical Science*, v. 15, n. 1, pp. 9568–9578, Aug. 2022.

[7] MARECI, D., NEMTOI, G.H., AELENEI, N., *et al*., "The electrochemical behavior non-precious Ni and Co based alloys in artificial saliva", *European Cells and Materials*, v. 10, pp. 1–7, 2005. https://www.ecmjournal.org/papers/vol010/pdf/v010a01.pdf, accessed in July, 2022.

[8] OH, K.-T., CHOO, S.U., KIM, K.M., *et al*., "A stainless steel Bracket for orthodontic application", *European Journal of Orthodontics*, v. 27, n. 3, pp. 237–244, Jun. 2005. doi: http://dx.doi.org/10.1093/ejo/cji005. PubMed PMID: 15947222.

[9] ADA COUNCIL ON SCIENTIFIC AFFAIRS, "Titanium applications in dentistry", *JADA*, v. 134, pp. 347–349, Mar. 2003.

[10] QUEZADA, E., DUFFÓ, G., "Corrosión de pares galvánicos de aleaciones dentales base cobre con amalgamas de plata en la cavidad oral", In: *Actas del Congreso CONAMET/SAM SIMPOSIO MATERIA 2002*, v. 1, pp. 407–411, Santiago de Chile, Nov. 2002.

[11] DUFFÓ, G.S., CASTILLO, E.Q., QUEZADA-CASTILLO, E., "Development of an artificial saliva solution for studying the corrosion behavior of dental alloys", *Corrosion*, v. 60, n. 6, pp. 594–602, Jun. 2004. http://dx.doi.org/10.5006/1.3287764

[12] QUEZADA-CASTILLO, E., "*Determinación de la susceptibilidad a la corrosión de aleaciones de uso odontológico*", Tesis de Maestría, Universidad Nacional de General San Martín y Comisión Nacional de Energía Atómica, Buenos Aires, Argentina, 1997.

[13] QUEZADA-CASTILLO, E., "*Corrosión de pares galvánicos de aleaciones dentales en la cavidad oral*", Tesis doctoral, Universidad General de San Martín y Comisión Nacional de Energía Atómica, Buenos Aires, Argentina 2004.

[14] MARECI, D., *et al*., "Electrochemical characterization of some copper based dental materials in accelerated test solutions", *Revista de Chimie*, v. 59, n. 8, pp. 871–877, 2008.

[15] MARECI, D., NEMTOI, G., AELENEI, N., *et al*., "The electrochemical behavior non-precious Ni and Co based alloys in artificial saliva", *European Cells & Materials*, v. 10, n. 1, pp. 1–7, discussion 1–7, 2005. PubMed PMID: 16003609.

[16] UNGUREANU, G., *et al*., "Pitting corrosion of a dental copper alloy in artificial saliva", *Scientific Study & Research*, v. 6, n. 2, pp. 197–204, 2005.

[17] BOHORQUEZ, C.E., "Galvanismo oral", *Revista Colombiana de Dermatología,* v. 6, n. 1, pp. 11–16, Mar. 1998.

[18] MUELLER, H.J., "Tarnish and corrosion of dental alloys", In: AST International Metal Park (ed), Metal Handbook, v. 13, Ohio, AST International Metal Park, pp. 1336–1366, 1992.

[19] PROCHÁZCOVA, C., *et al*., "Metal alloys in the oral cavity as a cause of oral discomfort in sensitive patients", *Neuroendocrinology Letters*, v. 27, s.1, pp. 53–58, Dec. 2006.

[20] BELTRÁN-CUEVAS, J., *et al*., "Carga eléctrica bucal desde una nueva perspectiva en estudiantes odontólogos de tres universidades: UANL, UV y Uagro", *Ciencia en la Frontera: Revista de Ciencia y Tecnología de la UACJ*, Supl. 1, pp. 97–106, 2021.

[21] AALBADENT. https://aalbadent.com/, accessed in Mayo, 2021.

[22] REQUENA CISNEROS, S.O., *et al*., "Adaptación de cofias metálicas confeccionadas con dos técnicas: cera perdida colada por centrifugación convencional e inducción", *Revista Estomatológica Herediana*, v. 29, n. 1, pp. 39–48, Jan-Mar. 2019.

[23] PETZOW, G., *Metallographic etching*, 2nd ed. Ohio, USA, ASM International, 1999.

[24] SHOESMITH, D.W., "Kinetics of aqueous corrosion", In: ASM International, Corrosion: Fundamentals, Testing and Protection, v. 13A, ASM Handbook, Ohio, ASM International, pp. 42–51, 2003.

[25] GEIS-GERSTROFER, J., PÄSSLER, K., "Studies on the influence of be content on the corrosion behavior and mechanical properties of Ni-25Cr-10Mo alloys", *Dental Materials*, v. 9, n. 3, pp. 177–181, May 1993. doi: http://dx.doi.org/10.1016/0109-5641(93)90117-9. PMid:8056173.

[26] ANGELINI, E., ZUCCHI, F., "In vitro corrosion of some Co-Cr and Ni-Cr alloys used for removable partial dentures: influence of heat treatments", *Journal of Materials Science Materials in Electronics*, v. 2, n. 1, pp. 27–35, 1991. doi: http://dx.doi.org/10.1007/BF00701684

[27] GIACCHI, J., *et al*., "Análisis microestructural de aleaciones Co-Cr-Mo para implantes", *Anales Alfa*, v. 20, pp. 194–199, 2008.

[28] SARKAR, N.K., FUYS JUNIOR, R.A., STANFORD, J.W., "Corrosion and microstructure of progold", *The Journal of Prosthetic Dentistry*, v. 40, n. 1, pp. 50–55, 1978. doi: http://dx.doi.org/10.1016/0022-3913(78)90158-0. PubMed PMID: 277684.

[29] BREZINA, P., "Heat treatment of complex aluminum", *International Metal Reviews*, v. 27, n. 1, pp. 77–120, 2013. doi: http://dx.doi.org/10.1179/imr.1982.27.1.77

[30] AMERICAN SOCIETY FOR TESTING AND MATERIALS. *G16-95 Standards Guide for Applying Statistics to Analysis of Corrosion Dat*. In: American Society for Testing and Materials, Anual Book of ASTM Standards, v. 3, New Jersey, West Conshohocken, Wiley, pp. 2, 1999.

[31] AMIGÓ BORRÁS, V., SALVADOR MOYÁ, M.D., FERRER GIMÉNEZ, C., "Fundamentos de corrosión y protección", In: Universidad Politécnica de Valencia, *Curso de Fundamentos de Ciencia de Materiales*, España, Universidad Politécnica de Valencia, pp.-xx–xx, 2001.

[32] REFAEY, S.A.M., TAHA, F., ABD EL-MALAK, A.M., "Corrosion and Inhibition of 316L stainless steel in neutral medium by 2-mercaptobenzimilazole", *International Journal of Electrochemical Science*, v. 1, pp. 80–91, May 2006.

[33] ARANGO-SANTANDER, S., LUNA-OSSA, C.M., "Stainless steel: material facts for the orthodontic practitioner", *Revista Nacional de Odontología*, v. 11, n. 20, pp. 71–82, 2015. doi: http://dx.doi.org/10.16925/od.v11i20.751

[34] BEKMURZAYEVA, A., DUNCANSON, W.J., AZEVEDO, H.S., *et al*., "Surface modification of stainless for biomedical applications: revisiting a century-old material", *Materials Science and Engineering C*, v. 93, n. 1, pp. 1073–1089, Dec. 2018. doi: http://dx.doi.org/10.1016/j.msec.2018.08.049. PubMed PMID: 30274039.

[35] SZALA, M., BEER-LECH, K., GANCARCZYK, K., *et al*., "Microstructural characterization of Co-Cr-Mo casting dental alloys", *Advances in Science and Technology Research Journal*, v. 11, n. 4, pp. 76–82, Dec. 2017. doi: http://dx.doi.org/10.12913/22998624/80901

[36] MOLINA, A., *et al*., "Metallographic characterization of overdenture bars fabricated by overcasting abutment for dental implants", *Revista Facultad de Odontología Universidad de Antioquia*, v. 25, n. 1, pp. 26–43, 2013.

[37] PORCOYO-CALDERON, J., *et al*., "Corrosion performance of Fe-Cr-Ni alloys in artificial saliva and mouthwash solution", *Bioinorganic Chemistry and Applications*, v. 2015, pp. 1–14. doi: https://doi.org/10.1155/2015/930802

[38] ANSARIFARD, E., FARZIN, M., ZOHOUR PARLACK, A., *et al*., "Comparing castability of nickel-chromium, cobalt-chromium, and non-precious golden color alloys, using two different casting techniques", *Journal of dentistry (Shīrāz, Iran)*, v. 23, n. 1, pp. 7–12, Mar. 2022. PMid:35291681.

[39] ROCHA ECHAVARRIA, O., *Introduccion a los biomateriales metálicos*, https://enlinea.zacatecas.tecnm.mx/pluginfile.php/28952/mod_resource/content/4/GUIA%20DE%20ESTU-DIO%20DE%20LA%20MATERIA%20DE%20INTRO%20A%20LOS%20BIOMATERIALES%20UNIDAD%20IV.pdf, accessed in July, 2022.

[40] MANSFELD, F., KENKEL, J.V., "Laboratory studies of galvanic corrosion of aluminium alloys in galvanic and pitting corrosion- field and laboratory studies", In: American Society for Testing and Materials, ASTM STP 576, New Jersey, West Conshohocken, Wiley, American Society for Testing and Materials, pp. 20–47, 1976.

[41] MANSFELD, F., "Area relationship in galvanic", *Corrosion*, v. 27, n. 1, pp. 436–442, 1971. doi: http://dx.doi.org/10.5006/0010-9312-27.10.436

[42] MANSFELD, F., "The relationship between galvanic current and dissolution rates", *Corrosion*, v. 29, n. 1, pp. 403–405, 1973. doi: http://dx.doi.org/10.5006/0010-9312-29.10.403